Popular Summary

A Comparison of Northern and Southern Hemisphere Cross-tropopause Ozone Flux

M. A. Olsen, A. R. Douglass and M. R. Schoeberl
Atmospheric Chemistry and Dynamics Branch
NASA Goddard Space Flight Center
Greenbelt, MD

The troposphere is the lowest layer of the atmosphere extending from the surface to an average midlatitude height of about 12 km. The tropopause separates the troposphere from the atmospheric layer immediately above called the stratosphere. Approximately 90% of atmospheric ozone is in the stratosphere. The remaining 10% is found primarily in the troposphere. The sources of ozone include pollution, chemistry, and transport from the stratosphere. Knowledge of how much tropospheric ozone results from each source is required to answer questions concerning the tropospheric composition, factors producing change in its composition, and interactions between upper tropospheric composition and climate.

A novel method of calculating the downward ozone flux across the midlatitude (30°-60°) tropopause shows the Northern Hemisphere (NH) ozone flux to be significantly larger ($\sim$ 24%) than that calculated in the Southern Hemisphere (SH) during the year 2000. This diagnostic method makes it possible to separate dynamical aspects of transport from the seasonal cycle of ozone in the lowermost stratosphere and explain the hemispheric difference in the ozone flux. The SH total horizontal area of exchange is equal to or slightly greater than the area of exchange in the NH throughout an annual cycle. The mean changes in potential vorticity of parcels near the tropopause are also similar or slightly greater in the SH, suggesting that NH and SH downward total mass transport to the troposphere are comparable. These results imply that the greater NH ozone flux is mostly due to the amount of ozone available for exchange rather than net hemispheric dynamical differences near the tropopause level.

A Comparison of Northern and Southern Hemisphere Cross-tropopause Ozone Flux

by

Mark A. Olsen

Anne R. Douglass

Mark R. Schoeberl

NASA Goddard Space Flight Center, Greenbelt, Maryland

Abstract

A novel method of calculating the downward ozone flux across the midlatitude (30°-60°) tropopause shows the Northern Hemisphere (NH) ozone flux to be significantly larger ($\sim$ 24%) than that calculated in the Southern Hemisphere (SH) during the year 2000. This diagnostic method makes it possible to separate dynamical aspects of transport from the seasonal cycle of ozone in the lowermost stratosphere and explain the hemispheric difference in the ozone flux. The SH total horizontal area of exchange is equal to or slightly greater than the area of exchange in the NH throughout an annual cycle. The mean changes in potential vorticity of parcels near the tropopause are also similar or slightly greater in the SH, suggesting that NH and SH downward total mass transport to the troposphere are comparable. These results imply that the greater NH ozone flux is mostly due to the amount of ozone available for exchange rather than net hemispheric dynamical differences near the tropopause level.

1. Introduction

Accurate estimates of stratosphere-troposphere exchange (STE) of ozone are necessary for robust studies of upper-tropospheric/lower-stratospheric chemistry and global climate. Our present knowledge of the ozone flux relies largely on 3D models [e.g., *Roelofs and Lelieveld*, 1995; *Tie and Hess*, 1997; *Hauglustaine et al.*, 1998; *McLinden et al.*, 2000]. Estimates of global ozone STE have also been made by extrapolating synoptic event results to global scales [e.g., *Lamarque and Hess*, 1994; *Beekmann et al.*, 1997]. Such extrapolation suffers from the heterogeny of synoptic scale events that transport different amounts of ozone due to dynamical and spatial differences. At best, a very large number of events would have to be analyzed to arrive at a reasonable ozone flux per event.

Appenzeller et al. [1996] show that the magnitudes of total mass exchanged in the extratropics of each hemisphere are not equal. Analysis of cross-tropopause ozone mass is further complicated by interhemispheric differences of lower stratospheric ozone mixing ratios [*Logan*, 1999]. In the present study, we examine the downward cross-tropopause transport of ozone at midlatitudes in both the Northern Hemisphere (NH) and Southern Hemisphere (SH). We use the STE diagnostic method of *Olsen et al.* [2002]. This method combines trajectory information with observed total column ozone data and is briefly presented in section 2. An advantage of the method is the ability to separate the dynamical aspects of cross-tropopause ozone transport from the temporally and spatially varying amount of ozone available for exchange.

2. Method of Analysis

Total ozone is found to be a linear function of column potential vorticity (PV) within 10° latitude bands in the midlatitudes. This linear relationship associates a difference in column ozone with the change in column PV (CPV). The CPV integration is from the tropopause to 70 hPa, the part of the stratosphere where ozone and PV are well correlated.

In this study we define the tropopause to be the 2 PVU surface (1 PVU = 10^{-6} m^2 K kg^{-1} s^{-1}).

We first calculate CPV from an analysis field. A second CPV field assuming PV conservation throughout the preceeding day is determined from 24 hour reverse domain filling (RDF) [*Sutton et al.*, 1994; *Newman and Schoeberl*, 1995]. The difference between the analysis CPV and that calculated using RDF reveals the tropopause movement relative to the parcels assuming processes leading to non-conservation of PV on a 24 hour time scale are always near the tropopause. Diabatic processes associated with irreversible transport, such as latent and radiative heating, destroy PV but do not change the ozone mixing ratio of air parcels. The amount of previously stratospheric ozone that has been left in the troposphere is then estimated by the product of the CPV difference and the linear relationship between column ozone and CPV.

Here we use total ozone data from the Earth Probe Total Ozone Mapping Spectrometer (EP/TOMS) [*McPeters et al.*, 1998] and PV and wind fields from the Goddard Earth Observing System Data Assimilation System Version 3 (GEOS DAS) [*DAO*, 2000]. Diabatic back-trajectories are calculated for a 3D grid of parcels, 0.5° longitude by 0.5° latitude and nine pressure surfaces (70, 100, 150, 200, 250, 300, 400, 500, and 700 hPa). Flux calculations for six days of each month (days 5, 12, 16, 20, 24, and 28) provide a good approximation for the monthly mean ozone flux [*Olsen et al.*, 2002]. Use of 72 days per year reduces the computational cost without significantly altering the results. We slightly modify the STE algorithm of *Olsen et al.* [2002] by including the first parcel level below the tropopause in the CPV calculations to better characterize the tropopause movement.

3. Results and Discussion

The midlatitude (30°-60°) ozone flux for the year 2000 is shown in Fig. 1. A late winter/early spring maximum and a late summer/early autumn minimum are observed in

each hemisphere (Fig. 1a). Figures 1b and 1c display the ozone flux within each 10° middle latitude band. The seasonal variability of each hemisphere is similar in the lower latitude bands but is greater in the SH than the NH from 50° to 60°. Month to month variability is greater at higher latitudes in both hemispheres. Shorter time scale variability is greater during the more baroclinically active winter and spring (Fig. 1a).

These results provide an estimate of the annual total downward ozone mass flux in the NH midlatitudes of 260 Tg yr^{-1} and 210 Tg yr^{-1} in the SH midlatitudes. The STE algorithm used in this study is only valid at midlatitudes and provides only a downward transport estimate, thus it is difficult to make direct comparisons with previous studies. However, $\sim$ 80-100% of the downward, cross-tropopause ozone flux in each hemisphere occurs equatorward of 60° [*Wang et al.*, 1998; *McLinden et al.*, 2000] and very little downward transport occurs in the tropical latitudes [*Holton et al.*, 1995]. Using a general circulation model with coupled chemistry, *Roelofs and Lelieveld* [1995] show a net global ozone flux of 575 Tg yr^{-1} with 59% in the NH. *Tie and Hess* [1997] use a chemistry transport model to find an extratropical ozone flux of 791 Tg yr^{-1} with 60% in the NH. *McLinden et al.* [2000] examine two ozone schemes, linearized ozone (linoz) where the chemical tendency of ozone is a linear function of temperature, ozone, and column ozone and synthetic ozone (synoz) where an inert tracer is released in the stratosphere at a fixed rate. Note that the synoz scheme prescribes the global net flux but does not constrain the flux to any particular latitudes. Using three sets of meteorological fields for each ozone scheme, they find that the linoz-derived net ozone flux equatorward of 60° ranges from 329 Tg yr^{-1} to 718 Tg yr^{-1} with 48% to 61% occurring in the NH. The synoz scheme results in a flux equatorward of 60° of 305 Tg yr^{-1} to 479 Tg yr^{-1} with 49% to 58% in the NH. The wide range of results from these previous studies illustrate the difficulty in determining the true ozone flux. Also, the interannual variability of ozone flux has not been examined in detail by previous studies. Our results of 470 Tg yr^{-1} of midlatitude ozone flux with 55% in the NH is reasonable compared with these 3D model-derived results.

Figure 2 shows the slope of the total ozone-CPV linear relationship for each month and 10° latitude band. The slopes reflect the ozone mixing ratio in the lower stratosphere [*Olsen et al.*, 2002]. Both hemispheres show a late winter/early spring maximum in all latitude bands. The NH winter maximum and summer minimum both exceed their SH counterparts, thus more ozone in the NH lower stratosphere is available for STE than in the SH for a given season. A climatology of ozonesonde data at 100 hPa [*Logan and McPeters*, 1999; G. Labow, personal communication, 2002] supports this assertion. For example, in the 40° to 50° latitude band the NH mean mixing ratio is $\sim$ 10% greater than in the SH during winter and $\sim$ 35% greater in the summer months (not shown).

The small slope values in the 50°S to 60°S latitude band during October and November are attributable to the SH ozone hole and transport of ozone-poor air to midlatitudes during its break-up. Plots of total ozone vs. CPV for these latitudes in October and November exhibit more spread of ozone values for a given CPV than other months (not shown). We note this as a caveat to the STE algorithm applied in the SH. During these months there can be two distinct air populations at the higher midlatitudes, air with "normal" ozone mixing ratios and ozone-depleted air. These air masses are poorly characterized by a simple linear relationship. Scatter invariably reduces the total ozone-CPV slope and the resulting STE estimate in this region will be subject to greater error.

We next examine the dynamical component of the downward ozone flux. The total horizontal area of active downward STE (summation of grid box areas where downward transport occurs) is shown in Fig. 3. The SH exhibits more seasonal variability with a winter maximum when summing over all midlatitudes. In the 30° to 40° latitude band the NH and SH magnitudes are comparable and have distinct seasonal cycles of winter maxima and summer minima. Between 40° and 50° there is little seasonal variation and both hemispheres have similar magnitudes. The greatest hemispheric differences are found

in the 50° to 60° latitude bands. There is little seasonal variation in the SH, but a seasonal cycle occurs in the NH with a summer maximum and a winter minimum.

The mean difference between analysis CPV and RDF CPV for the downward transport grid boxes is shown in Fig. 4 as a measure of the mean "depth" of STE. This "depth" of STE is not a direct measure of the change in tropopause height/pressure, though the movement of the tropopause relative to the parcels is implied. It is an indicator of the strength of the local PV-eroding processes. For example, weak (strong) diabatic processes will induce a small (large) CPV difference. The NH exhibits more seasonal variability of mean "depth" with a minimum in the summer months. This strong seasonal variability is not observed in the SH, and the SH mean "depth" remains nearly equal to or greater than the NH throughout the year.

The SH dynamical components of the STE algorithm, the area and "depth" of exchange, tend to be equal to or greater than the NH over an annual cycle. However, the mass of ozone exchange is greater in the NH. This is a result of more ozone near the midlatitude tropopause as shown by the total ozone-CPV slopes. From this we infer that the greater cross-tropopause ozone transport in the NH is caused by hemispheric constituent mixing ratio differences in the lowermost stratosphere rather than any near-tropopause dynamical differences.

Tie and Hess use a 3D chemistry transport model to examine the ozone budget between the 105 hPa and 290 hPa surfaces. They show that the magnitude of extratropical cross-tropopause ozone flux is controlled by wave driving in the stratospheric overworld. This conclusion is supported here. The near-tropopause dynamics govern the timing and location of the cross-tropopause ozone flux while the overworld wave driving ultimately dictates the magnitude.

Finally, we note that *Appenzeller et al.* [1996] show a slightly greater annual extratropical total mass flux across the 380 K surface in the NH than the SH. An equal or slightly greater SH total mass flux across the 2 PVU surface is implied here by the area of exchange and CPV differences. However, these two results are not directly comparable. *Appenzeller et al.* determine the net extratropical mass exchange while the results here are only the downward component from 30° to 60° in each hemisphere. In particular, significant isentropic upward and downward total mass transport occurs at extratropical latitudes less than 30° [e.g., *Chen*, 1995; *Dethof et al.*, 2000]. We also note that the *Appenzeller et al.* method is a bulk diagnostic that does not isolate the processes responsible for STE while diabatic exchange is inherently emphasized with the method used in the present study.

4. Conclusion

Downward midlatitude cross-tropopause ozone fluxes have been calculated for the year 2000 in both the NH and SH using assimilated winds and PV combined with TOMS total ozone observations. The midlatitude downward flux is found to be 260 Tg yr^{-1} in the NH and 210 Tg yr^{-1} in the SH. The seasonal variability of the midlatitude ozone STE is similar in both hemispheres except between 50° and 60° where the SH exhibits significantly greater seasonal-scale fluctuations. The greater flux of ozone to the NH troposphere is due to higher ozone mixing ratios near the NH tropopause, ultimately from hemispheric differences in stratospheric overworld wave driving.

ACKNOWLEDGMENTS

This work was completed while the first author held a National Research Council Research Associateship Award at Goddard Space Flight Center. Funding for this study was provided by NASA's EOS IDS program.

5. References

Appenzeller, C., J. R. Holton, and K. H. Rosenlof, Seasonal variation of mass transport across the tropopause, *J. Geophys. Res., 101*, 15071-15078, 1996.

Beekmann, M., G. Ancellet, S. Blonsky, D. De Muer, A. Ebel, H. Elbern, J. Hendricks, J. Kowol, C. Mancier, R. Sladkovic, H. G. J. Smit, P. Speth, T. Trickl, and Ph. Van Haver, Regional and global tropopause fold occurence and related ozone flux across the tropopause, *J. Atmos. Chem., 28*, 29-44, 1997.

Chen, P., Isentropic cross-tropopause mass exchange in the extratropics, *J. Geophys. Res., 100*, 16661-16673, 1995.

DAO, Algorithm Theoretical Basis Document, Version 2.00, Data Assimilation Office, NASA Goddard Space Flight Center, 2000.

Dethof, A., A. O'Neill, and J. Slingo, Quantification of the isentropic mass transport across the dynamical tropopause, *J. Geophys. Res., 105*, 12279-12293, 2000.

Hauglustaine, D. A., G. P. Brasseur, S. Walters, P. J. Rasch, J.-F. Müller, L. K. Emmons, and M. A. Carroll, MOZART, a global chemical transport model for ozone and related chemical tracers 2. Model results and evaluation, *J. Geophys. Res., 103*, 28291-28335, 1998.

Holton, J. R., P. H. Haynes, M. E. McIntyre, A. R. Douglass, R. B. Rood, and L. Pfister, Stratosphere-troposphere exchange, *Rev. of Geophys., 33*, 403-439, 1995.

Lamarque, J.-F. and P. G. Hess, Cross-tropopause mass exchange and potential vorticity budget in a simulated tropopause folding, *J. Atmos. Sci., 51*, 2246-2269, 1994.

Logan, J. A., An analysis of ozonesonde data for the lower stratosphere: Recommendations for testing models, *J. Geophys. Res., 104*, 16151-16170, 1999.

Logan, J. A., and R. D. McPeters, Ozone Climatology, in Models and Measurements II, edited by J.H. Park et al., Chap. 4, NASA Technical Memorandum 1999-209554, 307-362, 1999.

McLinden, C. A., S. C. Olsen, B. Hannegan, O. Wild, M. J. Prather, and J. Sundet, Stratospheric ozone in 3-D models: A simple chemistry and the cross-tropopause flux, *J. Geophys. Res., 105*, 14653-14665, 2000.

McPeters, R., P. K. Bhartia, A. Krueger, J. Herman, C. Wellemeyer, C. Seftor, G. Jaross, O. Torres, L. Moy, G. Labow, W. Byerly, S. Taylor, T. Swissler, and R. Cebula, Earth Probe Total Ozone Mapping Spectrometer (TOMS) Data Product User's Guide, NASA Technical Publication 1998-206895, 1998.

Newman, P. A., and M. R. Schoeberl, A reinterpretation of the data from the NASA stratosphere-troposphere exchange project, *Geophys. Res. Lett., 22*, 2501-2504, 1995.

Olsen, M. A., A. R. Douglass, and M. R. Schoeberl, Estimating downward cross-tropopause ozone flux using column ozone and potential vorticity, *J. Geophys. Res.*, in press, 2002.

Roelofs, G.-J., and J. Lelieveld, Distribution and budget of O_3 in the troposphere calculated with a chemistry general circulation model, *J. Geophys. Res., 100*, 20983-20998, 1995.

Sutton, R. T., H. Maclean, R. Swinbank, A. ONeill, and F. W. Taylor, High-resolution stratospheric tracer fields estimated from satellite-observations using Lagrangian trajectory calculations, *J. Atmos. Sci., 51*, 2995-3005, 1994.

Tie, X.-X., and P. Hess, Ozone mass exchange between the stratosphere and troposphere for background and volcanic sulfate aerosol conditions, *J. Geophys. Res., 102*, 25487-25500, 1997.

Wang, Y., J. A. Logan, D. J. Jacob, and C. M. Spivakovsky, Global simulation of tropospheric O_3-NO_x-hydrocarbon chemistry, 2. Model evaluation and global ozone budget, *J. Geophys. Res., 103*, 10727-10755, 1998.

Figure Legends

Figure 1 (a) Year 2000 downward cross-tropopause ozone mass flux in units of Tg day^{-1}. Bold lines are the monthly averages based upon 6 days per month for the NH (solid) and SH (dashed) midlatitudes. Thin lines are the flux for the 6 days each month. Panels (b) and (c) subdivide the magnitude of monthly mean ozone mass flux to 10° latitude bands in the (b) NH and (c) SH. The latitude bands are 30° to 40° (solid), 40° to 50° (dotted), and 50° to 60° (dashed).

Figure 2 Year 2000 seasonal variation of empirical slopes ($\Delta\Omega/\Delta PV^*$) for the NH (bold) and SH (thin) in the latitude bands of 30° to 40° (solid), 40° to 50° (dotted), and 50° to 60° (dashed).

Figure 3 The total horizontal area where cross-tropopause ozone flux is diagnosed from 30° to 60° (top bold line) in each hemisphere. Contributions from 30° to 40° (solid), 40° to 50° (dotted), and 50° to 60° (dashed) are shown.

Figure 4 The mean difference between the observed column PV and the RDF column PV where cross-tropopause ozone flux is diagnosed from 30°N to 60°N (solid) and 30°S to 60°S (dashed).

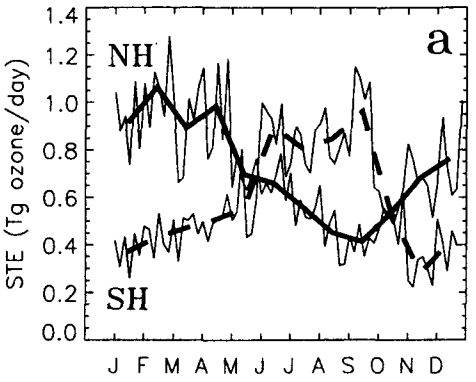

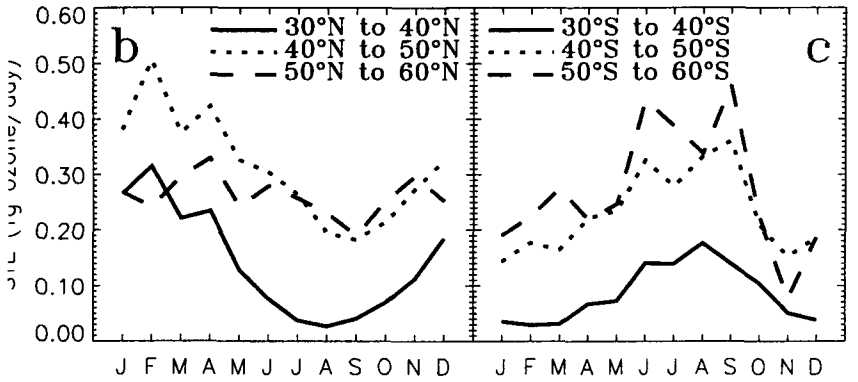

Figure 1

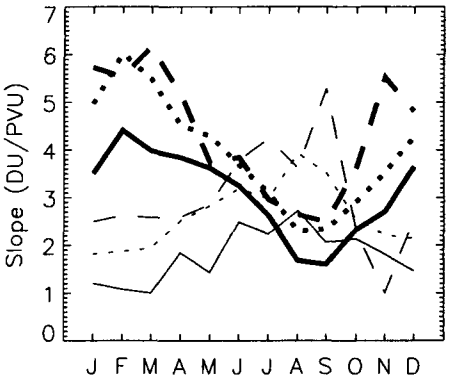

Figure 2

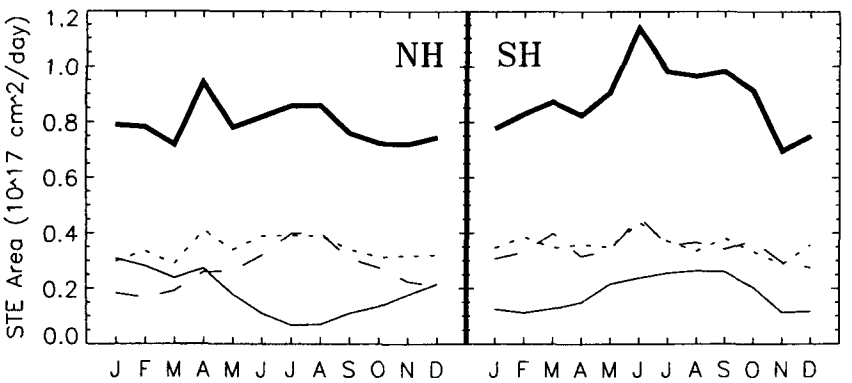

Figure 3

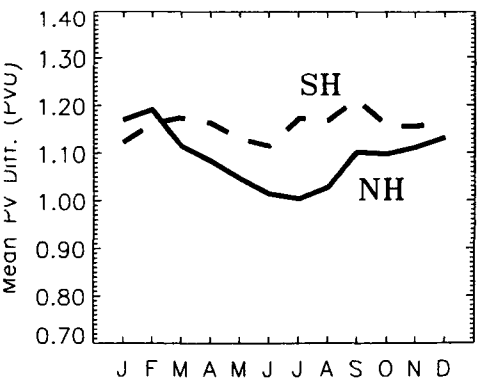

Figure 4